Journal of Luminescence 129 (2009) 6–11

Contents lists available at ScienceDirect

Journal of Luminescence

journal homepage: www.elsevier.com/locate/jlumin

Fluorescence properties of Ag nanoparticles in water, methanol and hexane

Om Parkash Siwach, P. Sen *

School of Physical Sciences, Jawaharlal Nehru University, New Delhi 110067, India

ARTICLE INFO

Article history:
Received 26 June 2007
Received in revised form
5 June 2008
Accepted 15 July 2008
Available online 26 July 2008

Keywords:
Ag nanoparticles
Electro-exploding wire
Fluorescence

ABSTRACT

Ag nanoparticles, synthesized employing the electro-exploding wire technique, are reported. Absorption in the UV–visible region by these particles is characterized by the features reported in the literature, namely, a possible plasmon peak at ~404 nm. For Ag nanoparticles dispersed in water, photo-excitation in the ranges 210–235 and 255–280 nm produces similar fluorescence emission at ~300 nm, whose corresponding resonant absorption takes place at 215 and 270 nm in the excitation spectra. Further, we study the effect of the surrounding medium (solvent effect) on fluorescence from these nanoparticles by comparing fluorescence emission in methanol and hexane for photo-excitation in the same range. Compared to water, fluorescence emission in methanol is observed red-shifted at ~310 nm, which further red-shifts to ~325 nm in hexane. The corresponding resonant absorptions in methanol are at 225 and 275 nm. Consequence of this red-shift in a less polar solvent is discussed.

1. Introduction

Noble metal nanoparticles continue to be of immense interest as they shed their inert character on size reduction [1–3], which demonstrate properties related to a high-aspect ratio and the quantum size effect [4]. Besides their ability to promote surface enhanced optical phenomenon [5,6], it was discovered that noble metal clusters display intense visible fluorescence. A study of fluorescence emitted from these particles, yields new insight into their origin and new application possibilities [1,7–9]. Fluorescence spectroscopy has proved as a very sensitive technique to study the fluorescence properties of nanoparticles.

Several techniques have been employed for the synthesis of noble metal nanoparticles, such as gas evaporation, arc plasma, sputtering, chemical reaction, electrochemical method, laser ablation [10–15] etc. Recently, an electro-exploding wire (EEW) technique has been established by us [16–19] for the preparation of metal nanoparticles, a process in which high currents are passed through a needle–plate geometry to synthesize nanoparticles.

An incident radiation interacts with metal electrons which result in basically one of the two following processes [20]. A plasma-type oscillation of the valence electrons, called plasmon oscillation and a dipole transition from a localized core level, creating a photo-hole. The photo-hole usually decays through transitions involving outer electrons, including the valence electron, to provide for characteristic photon emission called fluorescence.

Mooradian [21] observed fluorescence normal to noble metal surfaces for a glancing excitation (photon incidence angle ~10°) and reported broad fluorescence peaks centered near the inter-band absorption edge of the metals (2.0 and 2.2 eV for Cu and Au, respectively) for excitation at 488 nm from Cu and Au. The glancing incidence made the fluorescence preferentially emit from the surface atoms (a low dimensional system). Further, it was observed that at different excitation wavelengths (457.9–514.5 and 300–400 nm), the fluorescence peaked at the same energy and the high-energy tail increased slightly with higher photon energy pumping. The author assigned the observed fluorescence to transitions of electrons in the conduction band below the Fermi level to holes in the d bands. Recently, there are reports of fluorescence from Ag nanoparticles, which are bulk low dimensional systems, whereby several explanations are put forth. Jiang et al. [3] have reported fluorescence peak at 465 nm for Ag nanoparticles in water for excitation at 290 nm, and attributed it to interface electron energy band transitions. Basak et al. [22] have demonstrated shift in the fluorescence peak position towards longer wavelengths for Ag nanoparticles dispersed in PMMA matrix with increasing excitation wavelength in the range of ~370–550 nm. The speculation here is a resonance between the luminescence transition and silver plasmons, providing for the fluorescence. Treguer et al. [23] assigned fluorescence peaks observed at 550 and 700 nm for excitation at 300 and 350 nm, respectively, for Ag nanoparticles in aqueous medium, to the presence of oligomeric clusters of Ag_{4+x}^{x+} and Ag_7^{3+}. While, Jian et al. [14] reported two kinds of fluorescence peaks for Ag nanoparticles: one fixed at 315 nm, irrespective of the excitation

* Corresponding author. Tel.: +91 11 26704635; fax: +91 11 26717537.
E-mail address: psen0700@mail.jnu.ac.in (P. Sen).

0022-2313/$ - see front matter © 2008 Elsevier B.V. All rights reserved.
doi:10.1016/j.jlumin.2008.07.010

wavelength, assigned to local field enhancement and the other red-shifted from 540 to 595 nm with change in excitation wavelengths from 380 to 440 nm. The latter is speculated to arise due to electron interband transitions. Xu et al. [24] attributed fluorescence from Ag nanoparticles to metal to ligand charge transfer absorption.

In this paper, we report a detailed study of the fluorescence properties of silver nanoparticles dispersed in de-ionized water (hereafter referred to as water), methanol and hexane. Unlike previous reports, pure Ag nanoparticles, i.e., nanoparticles whose capping layers are synthesized as an extension of the metallic core, has been used for this study. The size obtained in TEM is in the range 8–20 nm while a small feature similar to a plasmon is still observed in UV–visible absorbance. The face centered cubic (FCC) nanoparticles dispersed in water exhibit a single fluorescence emission at 300 nm for excitation wavelengths (λ_{ex}) in both ranges 215–235 and 255–280 nm with resonant absorption at 215 and 270 nm respectively. While in methanol, the nanoparticles fluoresce with a singular emission at 310 nm for λ_{ex} in the ranges 210–235 and 265–285 nm; the corresponding resonant absorption take place at 225 and 275 nm, respectively. Further, the fluorescence of Ag nanoparticles dispersed in hexane is observed at 325 nm for λ_{ex} in the same range.

2. Experimental details

Ag nanoparticles reported here have been synthesized employing a novel, physical, top-down process of EEW. A schematic diagram of the EEW process has already been published by us [19]. In the EEW technique, a wire is exploded on a plate of the same material by passing a current density $\sim 10^{10}$ A/m^2, in a time $\sim 10^{-6}$ s. The wire-plate at the point of contact is heated due to the flow of high-density current, followed by melting. The melted metal at the point of contact is further heated by the ever-increasing current density due to increase in resistance, which leads to the evaporation of the material and subsequent plasma formation. This plasma is contained by the self-induced magnetic field. When the vapor pressure of the plasma overwhelms the self-induced magnetic field, explosion occurs and the plasma products are dispersed in the medium with high speed. Ag nanoparticles are thus synthesized by fragmentation of the parent material. Synthesized Ag nanoparticles are free from extraneous impurities, as no chemicals have been used in the nanoparticles synthesis. Parameters like current density, wire dimension and the medium in which explosion is carried out are monitored to have control over the entire process of exploding the wire [16–19]. The Ag nanoparticle powder is extracted by centrifugation.

XRD patterns were recorded on a Bruker D8 Advance diffractometer using CuK_α radiation ($\lambda = 1.5418$ Å). Further, the extracted Ag nanopowder is dispersed in methanol, hexane or water under ultrasonication. For TEM investigations a small drop of the diluted suspension was put on a carbon coated copper grid. After drying the grid, TEM characterization was carried out employing a JEOL JEM-2000EX transmission electron microscope. After ultrasonication (ultrasonicator power = 35 W) for 10 min, UV–visible absorbance spectrum was recorded of the Ag nanoparticles dispersed in water, on a Hitachi 3300 UV–visible double beam spectrophotometer, correcting the base line. With similar samples of Ag nanoparticles dispersed in water, hexane or methanol, fluorescence measurements have been carried out employing a Carey Eclipse fluorescence spectrophotometer from Varian, equipped with a Xenon light source and two Czerny-Turner monochromators for excitation and emission.

3. Results and discussion

XRD spectrum of the Ag nanoparticles is shown in Fig. 1a. There are peaks at $2\theta = 38.19^\circ$, 44.34°, 64.54° and 77.48° corresponding to reflections from the (1 1 1), (2 0 0), (2 2 0) and (3 1 1) planes, respectively. XRD peak position matches with that of bulk silver in FCC phase. So, the Ag nanoparticles, synthesized by EEW technique, exist in FCC phase. Fig. 1b shows the TEM image of the Ag nanoparticles. TEM analysis shows particle size in the range 8–20 nm. In Fig. 2, we show the UV–visible absorbance spectrum of the Ag nanoparticles dispersed in water. A peak at ~404 nm is reported to be a surface plasmon peak, due to collective oscillations of valence electrons in the electromagnetic field of the radiation and is characteristic of the Ag nanoparticles [22]. There are also weakly resolved absorption peaks at 260 and 213 nm, similar to those reported by others [22,25] and are due to transition of valence electrons to higher energy states.

It is well known that fluorescence is a three-step process involving the excitation of an electron from the ground state to high-energy states, followed by relaxation of the excited electron and finally fluorescence emission due to transition from the relaxed state to the ground state. Further, intensity of a transition (excitation/emission) peak depends upon the transition probability; highest intensity of a peak corresponds to maximum transition probability. If the frequency of radiation is ν, and ΔE is the energy difference between the two energy states, the transition probability is significant only when $h\nu = \Delta E$ in

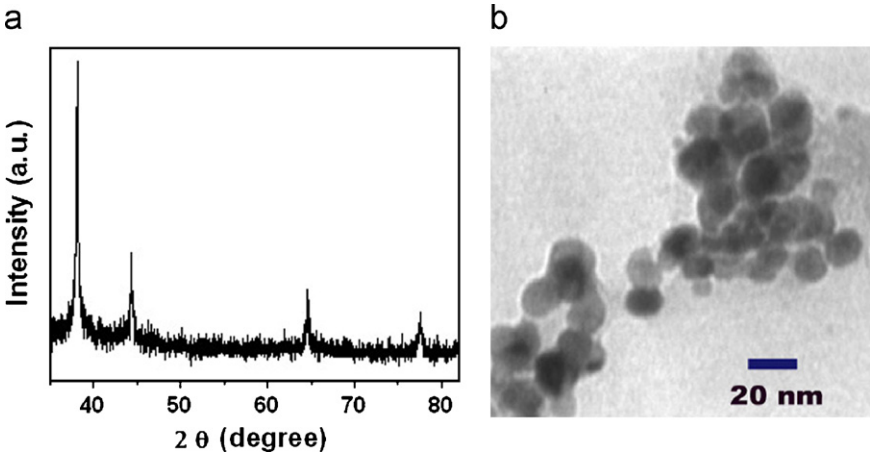

Fig. 1. (a) XRD pattern of the Ag nanoparticles and (b) TEM image of the Ag nanoparticles.

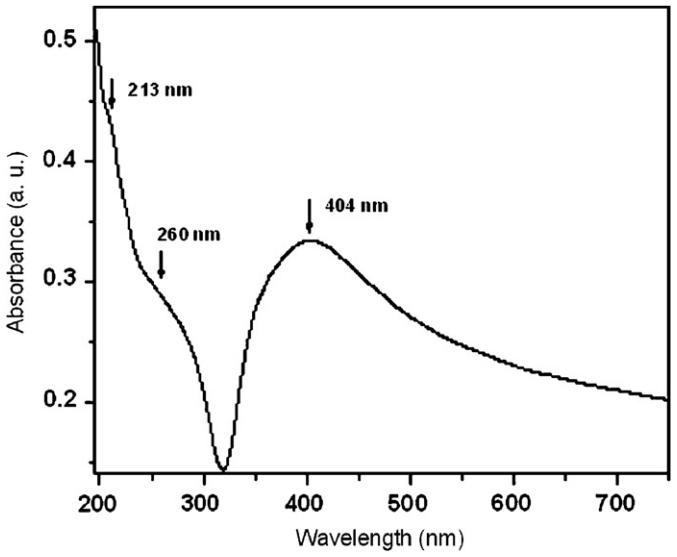

Fig. 2. UV–visible absorbance spectrum of the Ag nanoparticles dispersed in water.

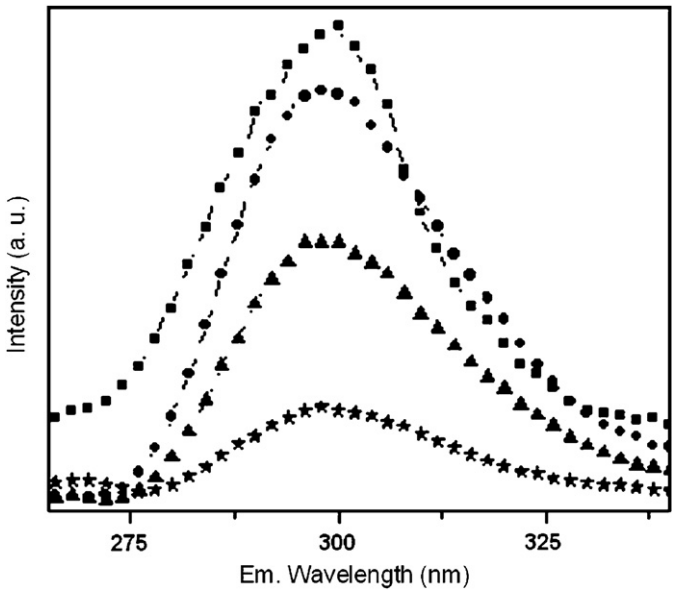

Fig. 3. Fluorescence emission spectra of Ag nanoparticles dispersed in water at $\lambda_{ex} = 215$ nm (squares), 225 nm (spheres), 230 nm (triangles) and 235 nm (stars).

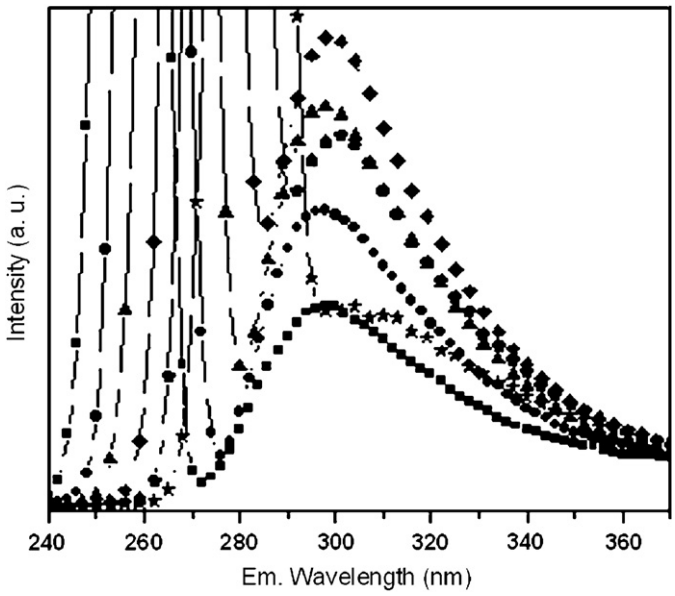

Fig. 4. Fluorescence emission spectra of Ag nanoparticles dispersed in water at $\lambda_{ex} = 255$ nm (squares), 260 nm (spheres), 265 nm (triangles), 270 nm (rectangles), 275 nm (pentagons) and 280 nm (stars).

accordance with the Fermi golden rule [26]. In corroboration of this, we show in Fig. 3, fluorescence emission spectra of the Ag nanoparticles dispersed in water (concentration of the Ag nanoparticles $\approx 2.5 \times 10^{17}$ atoms/cm^3) at $\lambda_{ex} = 215$ nm (squares), 225 nm (spheres), 230 nm (triangles) and 235 nm (stars). There are strong emission peaks at ~300 nm, the position of which remains approximately the same with change in λ_{ex}, and hence are assigned to fluorescence emission. The maximum fluorescence (as estimated from intensity of fluorescence peaks) is observed at $\lambda_{ex} = 215$ nm, decreasing thereafter with increase of λ_{ex}, which means that transition at $\lambda_{ex} = 215$ nm (5.67 eV) corresponds to the maximum transition probability. Further, Fig. 4 shows the fluorescence emission spectra of the Ag nanoparticles dispersed in water (concentration of the Ag nanoparticles $\approx 2.5 \times 10^{17}$ atoms/cm^3) for $\lambda_{ex} = 255$ nm (squares), 260 nm (spheres), 265 nm (triangles), 270 nm (rectangles), 275 nm (pentagons) and 280 nm (stars). Here too, fluorescence emission is observed at ~300 nm. The high-intensity peaks at 255, 260, 265, 270, 275 and 280 nm are Rayleigh scattering peaks, positions of which change with λ_{ex}. Rayleigh scattering lines have indeed been reported in conjunction with fluorescence emission from Ag nanoparticles in H_2O [3]. The fluorescence emission peak intensity at 300 nm increases as λ_{ex} increases, is maximum at $\lambda_{ex} = 270$ nm, and decreases thereafter as λ_{ex} increase. This indicates that resonant absorption/maximum transition probability is at $\lambda_{ex} = 270$ nm (4.59 eV) for Ag nanoparticles dispersed in water. To summarize, fluorescence of Ag nanoparticles in water is observed at 300 nm for both excitation ranges (a) 210–235 nm and (b) 255–280 nm.

When measuring the fluorescence of the Ag nanoparticles dispersed in a solvent, the most common state for the fluorescence measurements, it is important to note that the effect caused by the solvent are quite varied and complex [27]. In order to study the effect of the surrounding medium on fluorescence emission from the Ag nanoparticles, we recorded fluorescence emission of the Ag nanoparticles dispersed in methanol, at similar excitation wavelengths. In Fig. 5, we show the fluorescence emission spectra of the Ag nanoparticles dispersed in methanol (concentration of the Ag nanoparticles $\approx 2.5 \times 10^{17}$ atoms/cm^3) at $\lambda_{ex} = 210$ nm (squares), 220 nm (spheres), 225 nm (triangles), 230 nm (rectangles), 235 nm (stars), 240 nm (circles), 250 nm (pentagons). In case of Ag nanoparticles dispersed in methanol fluorescence emission peak is observed at ~310 nm, position of which remains fixed with change in λ_{ex}. Intensity of the fluorescence emission peak increases as the λ_{ex} increase, is maximum at $\lambda_{ex} = 225$ nm, and decrease thereafter as the λ_{ex} increase. Maximum fluorescence emission intensity at $\lambda_{ex} = 225$ nm indicates that $\lambda_{ex} = 225$ nm corresponds to maximum transition probability/resonant absorption for Ag nanoparticles dispersed in methanol. Further, Fig. 6 shows the fluorescence emission spectra of the Ag nanoparticles dispersed in methanol (concentration of the Ag nanoparticles $\approx 2.5 \times 10^{17}$ atoms/cm^3) at $\lambda_{ex} = 255$ nm (squares), 260 nm (pentagons), 265 nm (rectangles), 270 nm (spheres), 275 nm (triangles), 285 nm (circles) and 290 nm (stars). Here too, fluorescence peak is observed at ~310 nm. The intensity of the fluorescence emission peak again goes through a maximum at $\lambda_{ex} = 275$ nm, corresponding to maximum transition probability for Ag nanoparticles dispersed in methanol. There are also strong peaks at

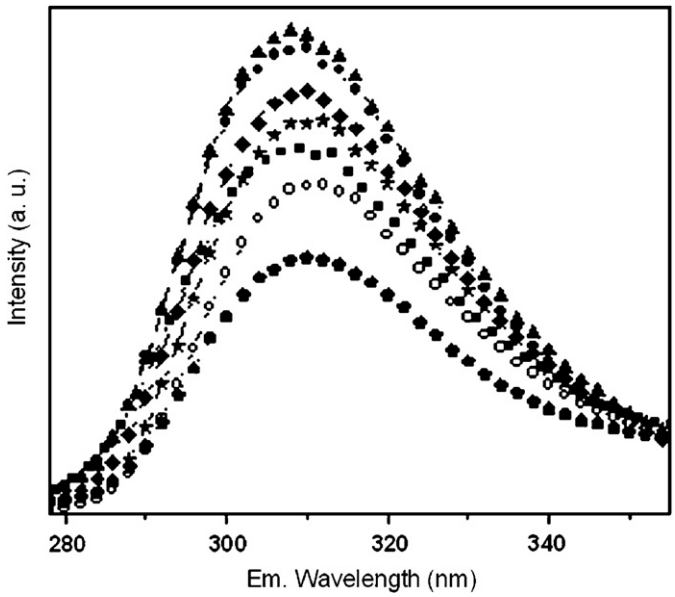

Fig. 5. Fluorescence emission spectra of Ag nanoparticles dispersed in methanol at $\lambda_{ex} = 210$ nm (squares), 220 nm (spheres), 225 nm (triangles), 230 nm (rectangles), 235 nm (stars), 240 nm (circles) and 250 nm (pentagons).

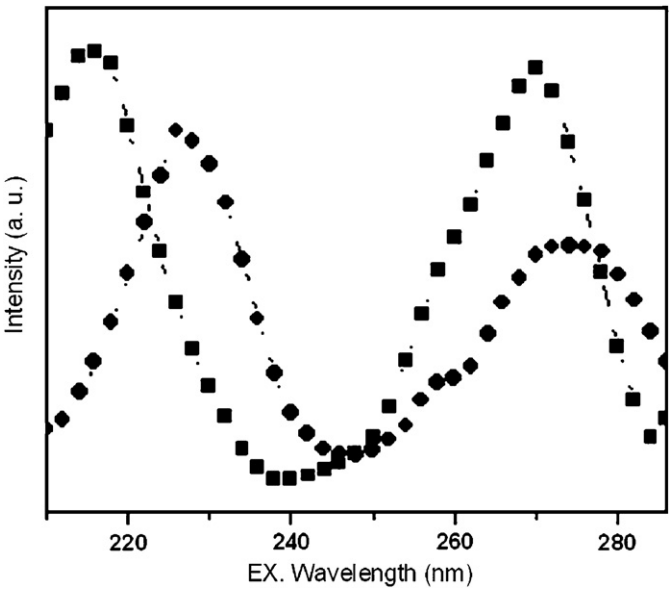

Fig. 7. Fluorescence excitation spectra of Ag nanoparticles (concentration of the Ag nanoparticles $\approx 2.5 \times 10^{17}$ atoms/cm^3) dispersed in water for λ_{em} fixed at 300 nm (squares) and of Ag nanoparticles dispersed in methanol for λ_{em} fixed at 310 nm (spheres).

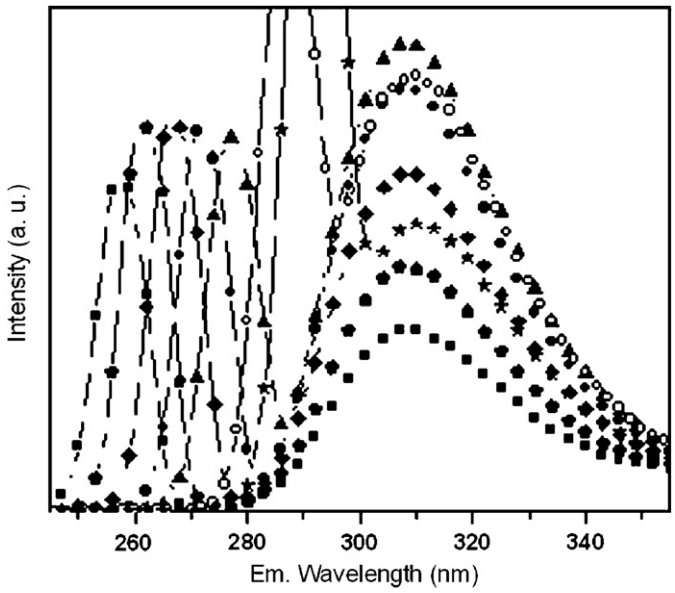

Fig. 6. Fluorescence emission spectra of Ag nanoparticles dispersed in methanol at $\lambda_{ex} = 255$ nm (squares), 260 nm (pentagons), 265 nm (rectangles), 270 nm (spheres), 275 nm (triangles), 285 nm (circles) and 290 nm (stars).

255, 260, 265, 270, 275, 285 and 290 nm, which are Rayleigh scattering peaks, as discussed previously. To summarize, as for water earlier, similar fluorescence emission is observed at the same position ~310 nm of the Ag nanoparticles dispersed in methanol for λ_{ex} in the ranges (a) 210–250 nm and (b) 255–290 nm. However, the primary difference in emission of the nanoparticles in water and methanol is in the position of the emission which is red-shifted in the latter.

Shift in the emission peak position due to a solvent's dielectric constant has been well researched in the literature [27] and is known to provide polarization shifts. Thus the red-shift in methanol is unexpected as methanol is a relatively non-polar solvent compared to water (dielectric constant of water is 80.3 and of methanol is 33.6). Also, a shift per se may not mean much if this is not compared with the excitation peak position. Polarization shifts take place when energy absorbed during excitation is lost from the fluorophore due to the availability of other channels in its immediate surrounding, namely, the solvent molecules.

We now proceed to measure the exact location of the absorption maxima by recording the excitation spectra of the Ag nanoparticles dispersed in water or methanol with fluorescence emission wavelength (λ_{em}) fixed at the location where highest intensity of the fluorescence peak is observed. Fig. 7 shows the fluorescence excitation spectra of the Ag nanoparticles dispersed in water (squares) for λ_{em} fixed at 300 nm and in methanol (spheres) for λ_{em} fixed at 310 nm. The excitation spectrum in water is marked by two broad peaks centered at ~215 and ~270 nm. This indicates excitation in Ag nanoparticles to energy levels corresponding to energy of these peaks. Intensity of these peaks is maximum at ~215 and ~270 nm, corresponds to maximum transition probability. Hence, the resonant absorption in Ag nanoparticles dispersed in water takes place at $\lambda_{ex} = 215$ and 270 nm. This resonant absorptions/maximum transition probabilities are also corroborated by the fluorescence emission spectra, where intensity of the fluorescence peaks of the Ag nanoparticles dispersed in water is maximum at $\lambda_{ex} = 215$ nm, decreases as excitation wavelength increases, and attain a maximum at $\lambda_{ex} = 270$ nm, corresponding to a second resonant absorption. In the excitation spectrum of the Ag nanoparticles dispersed in methanol, there are peaks at ~225 and ~275 nm, corresponding to maximum transition probabilities. This is in conformity with the fluorescence emission data, where intensity of fluorescence peak of Ag nanoparticles dispersed in methanol is maximum at $\lambda_{ex} = 225$ and 275 nm.

A red-shift of 10 nm in fluorescence from the nanoparticles in methanol, a less polar solvent compared to water, can now be commented upon. In a polarization shift scenario, the excitation peak holds its position, while the emission shifts. This is in accordance with the access to other energy loss pathways, namely reorientation of solvent molecules by the fluorophore through dipolar interactions. However, evidence of such energy loss is absent here as the separation between emission and excitation

remains constant. Thus the observed shift has its origin somewhere else.

In the region of fluorescence emission observed by us (i.e., at ~300 nm), a peak at 315 nm has been reported by Jian et al. [14] for Ag nanoparticles who attributed its origin to local field enhancement, whereas Mooradian [21] attributed the observed fluorescence from noble metals to transitions of electrons in the conduction band below the Fermi level to holes in the d bands. Also, fluorescence from Au nanoparticles has been attributed to interband electronic transitions between the $6sp^1$ conduction band and $5d^{10}$ valence levels [28]. For noble metal nanoparticles, it is well known that the energy band will split into a series of energy levels in terms of the quantum size effect. Further, the splitting of energy levels will be more distinct as the size of the nanoparticles becomes smaller. The relationship between level spacing (δ) and particle size is given by $\delta = 4E_F/(3N)$, where E_F denotes the Fermi energy, N denotes the number of conduction electrons or $\delta \propto 1/d^3$, where d is particle size (for a spherical particle) [4,29]. So the energy level splitting makes the electronic transition abundant. It is known as a general rule in fluorescence that a molecule deexcites to the lowest vibrational level of its lowest excited state prior to photon emission [27], in a time short enough compared to photon emission times. Our careful λ_{ex} dependence study of fluorescence allows us to however assign these to transitions to various excited states from the d levels of the Ag nanoparticles, in accordance with the data presented in Figs. 3–7. The deexcitation however takes place from the lowest excited state, to provide similar fluorescence emission wavelengths for different absorption manifolds.

In conformity with the fluorescence emission observed, we show in Fig. 8, a schematic diagram showing energy levels in order to describe the fluorescence mechanism operating in the Ag nanoparticles. Electrons excitation takes place from 4d to various excited states, depending upon the excitation energy. The upward transition from the d level of Ag nanoparticles to the excited states are marked by thick arrows and their labels, namely, UP1 and UP2 are marked next to these arrows. Also marked is the downward transition taking place from the bottom of the first excited state, which gives rise to the fluorescence emission (DN1). The difference between UP1 and the fluorescence emission energy observed is due to Stokes Shift i.e. due to vibrational relaxation after absorption and after fluorescence emission. The second excited state is achieved through an upward transition UP2 as shown in Fig. 8. However, here UP2 deexcites via DN2, also shown in Fig. 8, which is possible only through a transition or a major reorganization DN*. A measure of the width of the second excited state as well as the presence or absence of DN* cannot be verified, as we have no possibility of detection of radiation emanating with an energy of 1.2 eV. Fluorescence emission take place when excited electrons, after relaxation, are deexcited back to the 4d levels. A level scheme (dotted lines) based on absorption in and emission from the Ag nanoparticles in methanol is shown here too.

Metal to ligand charge transfer and electron interband transitions have been put forth in the literature [14,24] to explain fluorescence from Ag nanoparticles. These reports however lacked the possibility of observing fluorescence from pure nanoparticles, substantially smaller, as reported here. This has allowed us the identification of fluorescence peaks which are considerably narrow and hence allow tracking minor shifts. The proposal for fluorescence emission put forth in Fig. 8 is a result of such a capability. Together with monitoring fluorescence shifts we have also identified the lack of correlation with polarization shifts in the presence of solvents. Thus the shifts observed need to be based on an independent origin. If the nanoparticle atoms are considered as having an effective central potential with an effective positive charge Z_{eff}, any charge transfer from the metal to a ligand will stabilize the electronic levels (due to an increase in Z_{eff}). This will include the excited states. From photoemission studies [30] involving water and methanol adsorption on metallic surfaces, a larger charge transfer from the metal is observed in the case of water as compared to methanol. Thus if the excited states depicted in Fig. 8 were to be on the metal site, a greater stabilization of these levels would ensue in the case of water. We however find just the opposite.

We thus propose the origin of the excited states to electronic states at the surface of the nanoparticle in the central potential Z_{eff}/R of the nanoparticle atom, where R is the radius of the nanoparticle. In the presence of molecules such as water, with which hybridization of such electronic states are possible, these are destabilized due to the involvement of the ligand states through the exchange term. Under this description, a ligand which is expected to be least hybridized to the nanoparticle would produce the most stable excited state. We indeed find such a situation when fluorescence of the nanoparticles is measured in the presence of hexane, a non-polar solvent. Fig. 9 shows the fluorescence emission spectra of the Ag nanoparticles dispersed in hexane

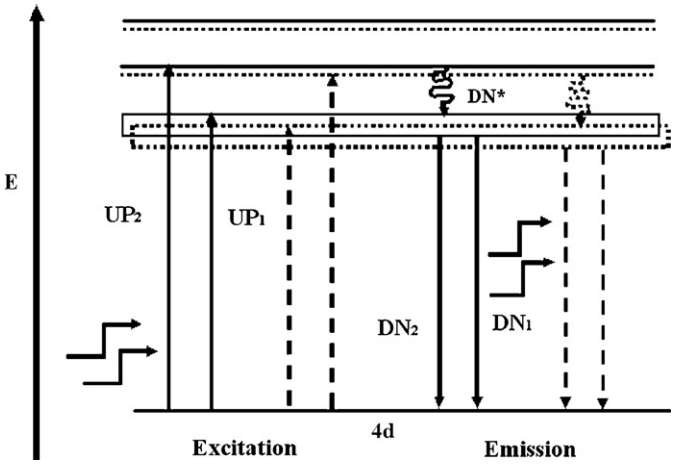

Fig. 8. Schematic energy level diagram for fluorescence mechanism of the Ag nanoparticles.

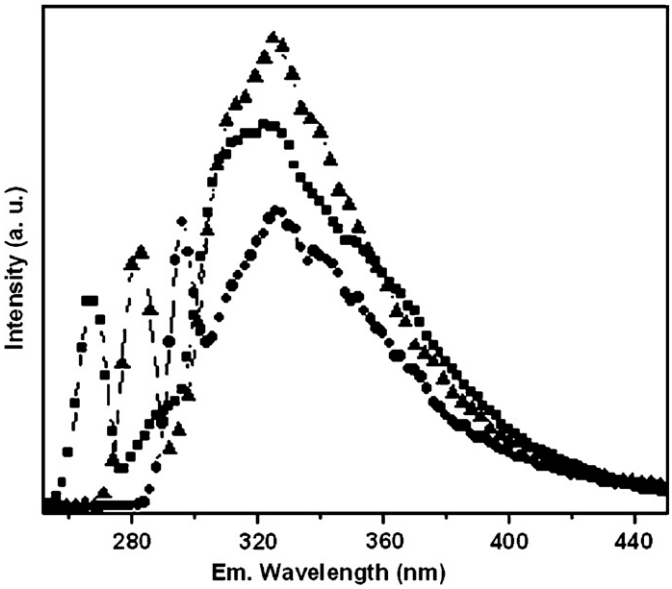

Fig. 9. Fluorescence emission spectra of Ag nanoparticles dispersed in hexane at $\lambda_{ex} = 265$ nm (squares), 280 nm (triangles) and 295 nm (spheres).

(concentration of the Ag nanoparticles $\approx 2.5 \times 10^{17}$ atoms/cm^3) at $\lambda_{ex} = 265$ nm (squares), 280 nm (triangles) and 295 nm (spheres). High-intensity peaks at 265, 280 and 295 nm are Rayleigh scattering peaks, and the peaks at ~325 nm are fluorescence emission peaks of the Ag nanoparticles dispersed in hexane, as already established. The fluorescence emission is further red-shifted to 325 nm as compared to methanol (at 310 nm).

4. Conclusions

We have successfully demonstrated fluorescence emission from Ag nanoparticles prepared by electro-explosion of wires. These particles, bereft of external capping through organic ligand groups, show specific fluorescence emission in presence of water, methanol and hexane at 300, 310 and 325 nm, respectively. The fluorescence emission is similar, namely involve absorption via two excited states which after reorganization deexcite through the lowest excited state. This is a novel result and is specific to nanoparticles. Also, our preliminary results further demonstrate the ability of this technique to identify various solvents in the immediate surrounding of the nanoparticles, which now behave like a nanoparticle with atom-like features.

Acknowledgments

The authors thank the School of Life Sciences, Jawaharlal Nehru University for allowing use of the fluorescence spectrophotometer. One of us (OP) thanks CSIR, India for a research fellowship.

References

[1] L.A. Peyer, A.E. Vinson, A.P. Bartako, R.M. Dickson, Science 291 (2001) 103.
[2] J.P. Wilcoxon, J.E. Martin, F. Parsapour, B. Wiedenman, D.F. Kelley, J. Chem. Phys. 108 (1998) 9137.
[3] Z. Jiang, W. Yuan, H. Pan, Spectrochim. Acta A 61 (2005) 2388.
[4] N. Nilius, N. Ernst, H.J. Freund, Phys. Rev. Lett. 84 (2000) 3994.
[5] W.E. Doering, S. Nie, J. Phys. Chem. B 106 (2002) 311.
[6] S. Nie, S.R. Emory, Science 265 (1997) 1102.
[7] N. Pinna, M. Maillard, A. Courty, V. Russier, M.P. Pileni, Phys. Rev. B 66 (2002) 045415.
[8] H. Geerts, M. de Brabander, R. Nuydens, Nature 351 (1991) 765.
[9] J.F. Hainfeld, R.D. Powell, J. Histochem. Cytochem. 48 (2000) 471.
[10] G.T. Fei, R. Lu, Z.J. Zhang, G.S. Cheng, L.D. Zhang, P. Cui, Mater. Res. Bull. 32 (1997) 603.
[11] K. Ohsaki, X.G. Li, Mater. Sci. Eng. A 252 (1999) 141.
[12] C. Charton, M. Fahland, Surf. Coat. Technol. 174–175 (2003) 181.
[13] N. Shirtcliffe, U. Nickel, S. Schneider, J. Colloid Interf. Sci. 211 (1999) 122.
[14] Z. Jian, Z. Xiang, W. Yongchang, Microelectron. Eng. 77 (2005) 58.
[15] F. Mafune, Jun-ya Kohno, Y. Takeda, T. Kondow, H. Sawabe, J. Phys. Chem. B 104 (2000) 9111.
[16] P. Sen, J. Ghosh, A. Abdullah, P. Kumar, Vandana, Proc. Indian Acad. Sci. (Chem. Sci.) 115 (2003) 499.
[17] N. Goswami, P. Sen, Solid State Commun. 132 (2004) 791.
[18] Om Parkash, P. Sen, Material Research Society Symposium Proceedings, vol. 900E, 0900-O03-31.1, 2006.
[19] Vandana, P. Sen, J. Phys: Condens. Matter 17 (2005) 5326.
[20] B.M. Smirnov, H. Weidele, J. Exp. Theor. Phys. 89 (1999) 1030.
[21] A. Mooradian, Phys. Rev. Lett. 22 (1968) 185.
[22] D. Basak, S. Karan, B. Mallik, Chem. Phys. Lett. 420 (2006) 115.
[23] M. Treguer, F. Rocco, G. Lelong, A.L. Nestour, T. Cardinal, A. Maali, B. Lounis, Solid State Sci. 7 (2005) 812.
[24] Jian Xu, Xia Han, Honglai Liu, Ying Hu, Colloid Surf. A: Physicochem. Eng. Aspects 263 (2006) 179.
[25] T. Kim, Y.W. Kim, J.S. Kim, B. Pank, J. Mater. Res. 19 (2004) 1402.
[26] A.K. Ghatak, S. Loknathan (Eds.), Quantum Mechanics: Theory and Applications, Macmillan India Ltd., India, 1984.
[27] D.M. Hercules, Fluorescence and Phosphorescence Analysis: Principles and Applications, Interscience Publishers, New York, 1966.
[28] T. Huang, R.W. Murray, J. Phys. Chem. B 105 (2001) 12498.
[29] W.P. Halperin, Rev. Mod. Phys. 58 (1986) 533.
[30] P. Sen, C.N.R. Rao, Surf. Sci. 172 (1986) 279.